

Polymerizable UV absorbers for the UV stabilization of polyesters. II. Photodegradation study of UV-stabilized PET copolymers

Peter A. G. Cormack,^{*a} Omer C. Erdemli,^a and Stephen W. Sankey^b

^aWestCHEM, Department of Pure and Applied Chemistry, University of Strathclyde, Thomas Graham Building,
295 Cathedral Street, Glasgow, G1 1XL, Scotland, UK

^bDuPont Teijin Films UK Limited, Wilton, Middlesbrough, TS10 4RF, England, UK

E-mail: Peter.Cormack@strath.ac.uk

Dedicated to Professor Phil Hodge for his outstanding lifetime achievements in organic and polymer chemistry

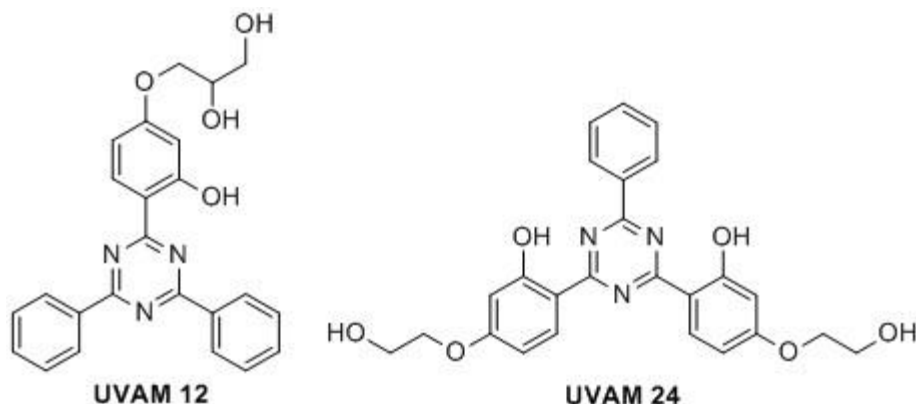
Received 08-16-2021

Accepted 11-23-2021

Published on line 12-10-2021

Abstract

Polymerizable UV absorbing monomers (UVAMs) were copolymerized with *bis*(hydroxyethyl) terephthalate to yield copolymers of poly(ethylene terephthalate) (PET). PET copolymer films containing 3-[4-(4,6-diphenyl-1,3,5-triazin-2-yl)-3-hydroxyphenoxy]-1,2-propanediol (UVAM **12**) and 6,6'-(6-phenyl-1,3,5-triazine-2,4-diyl)*bis*(3-(2-hydroxyethoxy)phenol) (UVAM **24**) were exposed to UV radiation for 1082 hrs. in a QUV-A accelerated weathering instrument and analyzed periodically using FT-IR spectroscopy and GPC. It was found that PET films containing copolymerized UVAMs outperformed films containing admixed Tinuvin 1577 stabilizer, thereby offering even greater protection to polymer films against UV-induced crosslinking and chain scission.



Keywords: Ultraviolet, degradation, poly(ethylene terephthalate), UV absorber, Tinuvin 1577

Introduction

Poly(ethylene terephthalate) (PET) absorbs strongly in the ultraviolet (UV) region of the EM spectrum (Figure 1) and this leads to the photodegradation of polymer chains. UV stabilizer additives are employed to prevent the UV-induced photodegradation of polyester films, especially for those applications where the levels of UV exposure of the polymer films is high, *e.g.*, photovoltaic cells.¹ One limitation concerning the use of UV stabilizers is the loss of additive from the polymer over time by leaching. One way in which this problem can potentially be overcome is to tether the UV stabilizers to the polymer chains by stable covalent bonds.²

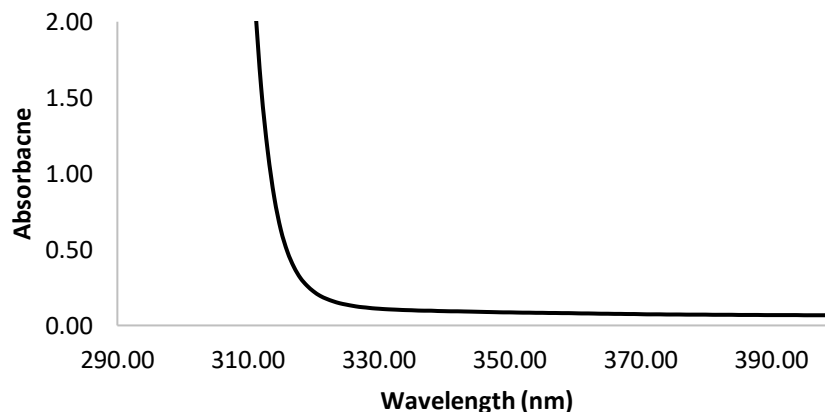


Figure 1. UV absorbance spectrum of a PET film.

UV degradation of PET

The photochemistry of polyester degradation is a complex area and has been studied extensively over the past fifty years. In the early 1970s, Day and Wiles³⁻⁶ proposed mechanisms (Figure 2) to explain the formation of the three main products (-COOH, CO and CO₂) arising from the exposure of PET to oxidative and non-oxidative conditions. It was found that wavelengths below 310 nm were critical for main-chain scission and that wavelengths above 315 nm led to the production of COOH end groups. Day and Wiles postulated that carboxylic acid end groups were formed by a Norrish Type II photo-elimination reaction involving an intramolecular rearrangement of the ester group into an olefin and carboxylic acid. CO build-up was explained by a photolytic chain-scission, a Norrish Type I reaction. The rate of CO₂ formation increased dramatically for irradiations conducted in the presence of air, suggesting that oxygen played a role in the process. Furthermore, the hydroxyl radicals formed could give rise to the fluorescent mono-/di-hydroxyl terephthalate species.

Fechine⁷⁻⁹ proposed an alternative mechanism involving a Norrish Type I reaction which proceeded through a radical pathway in the presence of oxygen, and Rivaton *et al.*¹⁰ reported further oxidation of the aldehydes to produce additional carboxylic acid end groups.

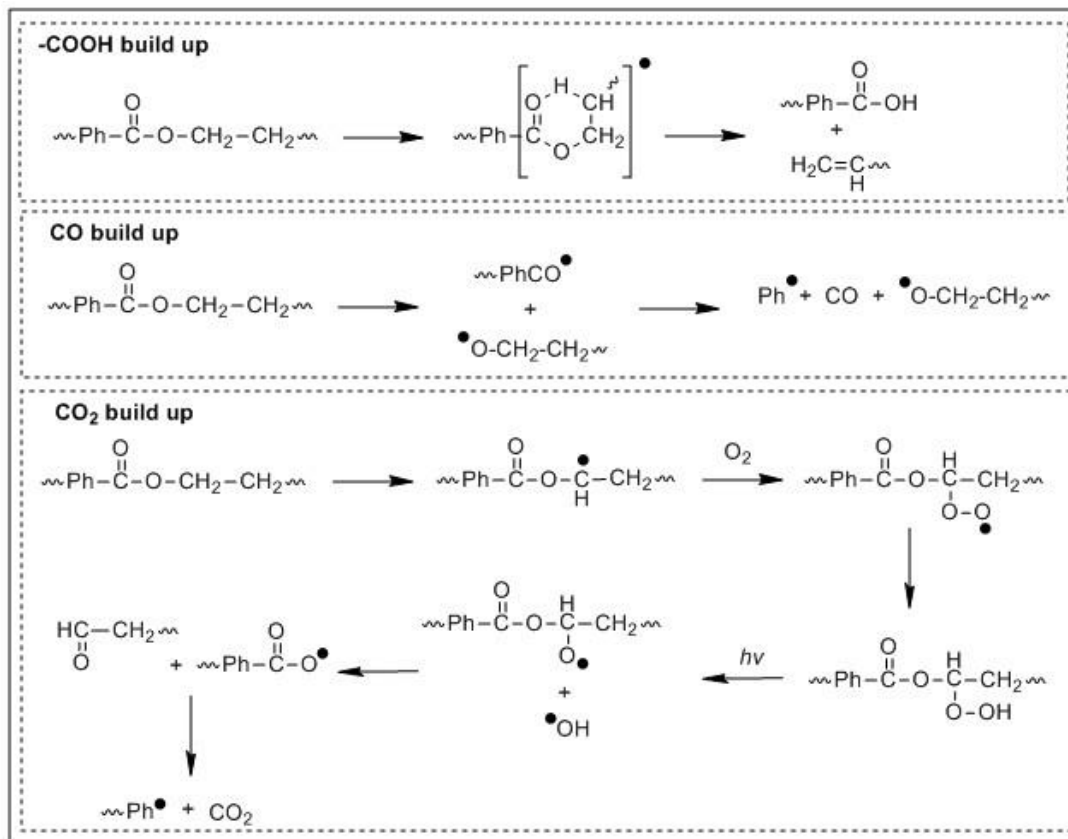


Figure 2. Mechanisms proposed by Day and Wiles for the formation of –COOH, CO and CO₂ during the photodegradation of PET.⁵

Ultraviolet absorbers

Ultraviolet absorbers (UVAs) are commercially available polymer additives that are employed commonly in the polymer industry due to their effectiveness in protecting polymeric materials from UV radiation. They absorb UV light and dissipate the UV energy into harmless heat energy whilst remaining chemically unchanged through a process called excited state intramolecular proton transfer (ESIPT).^{11–13} ESIPT is observed with planar 5- and 6-membered rings that have intramolecular hydrogen bonding (IMHB) between a phenolic hydrogen and a heteroatom. The heteroatom is normally either a nitrogen atom, from 2-(hydroxyphenyl)benzotriazole^{14,15} (BT) or 2-(2-hydroxyphenyl)-1,3,5-tiazine (TA) derivatives,² or an oxygen atom from 2-hydroxybenzophenone (BP) or salicylate derivatives.¹⁶

Tinuvin 1577 (Figure 3) is the leading UVA available on the market today.^{17,18} This TA derivative is manufactured by BASF and is currently the UVA of choice for DuPont Teijin Films (DTF) as an additive for PET. As well as being a powerful UV screen, Tinuvin 1577 exhibits a robust IMHB, it is resilient to polar environments and it has a low yellowing index.^{7,9,17,18}

One major limitation concerning the use of Tinuvin 1577, and essentially all other UVAs, is the potential leaching of the stabilizer from the polymer matrix. The loss of additive over time leads to an increase in the rate of UV-induced degradation and deterioration of key polymer properties. This is of particular concern for applications where polymers are exposed to high levels of UV radiation and/or conditions that allow leaching of additives from the polymers. It is of the utmost importance for polymer manufacturers to increase the lifetime of UV protection, and one way in which this can potentially be achieved is by exploiting polymerizable UVAs which are bonded covalently to the polymer chains. In this way, copolymerized UVAs comprise an integral part

of the polymer structure, and this may prolong the lifetime of UV protection and perhaps enhance the level of UV protection as well.

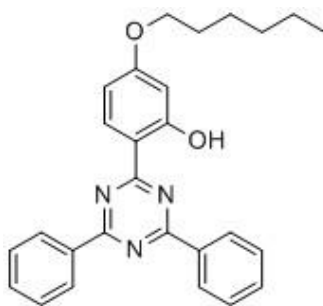


Figure 3. Tinuvin 1577.

There has been extensive work on the preparation of UVAs bearing vinyl functionality, especially BP and BT derivatives, for copolymerization through free radical polymerization routes.^{19–24} More recent studies by Kramer *et al.* described the synthesis of TAs with vinyl moieties and the free radical copolymerization of the same with styrene and methyl methacrylate.^{2,25} Recent work by Bojinov^{26–33} involved the synthesis of various polymerizable ultraviolet stabilizers with a variety of functionalities. Several of Bojinov's compounds contained both a UVA moiety and a photo-antioxidant fragment.

There are many fewer examples of polymerizable UVAs copolymerized *via* step-growth polymerization processes as compared to free radical polymerization. Bailey and Vogl^{23,24} copolymerized BPs to yield polyamide copolymers. In addition to preventing leaching, Bailey and Vogl reported that polymerized UVAs reduce volatilization and the spectral profiles remained unchanged by polymerization. Kulia *et al.* copolymerized BTs with phenolic moieties in a step-growth polymerization to yield polysulfone and polycarbonate copolymers.¹⁵

Results and Discussion

In the first paper in this series, we disclosed the synthesis of UVAMs **12** and **24** (Figure 4) and their copolymerization into polyesters. The UVAMs were prepared using cyanuric chloride as the synthetic starting point, and Grignard and Friedel-Crafts chemistries were used to build the main chromophore framework of these compounds. The polymerizable moieties were installed *via* nucleophilic aliphatic substitutions with 2-bromoethanol and 3-chloropropane-1,2-diol to yield UVAMs **12** and **24**, respectively.

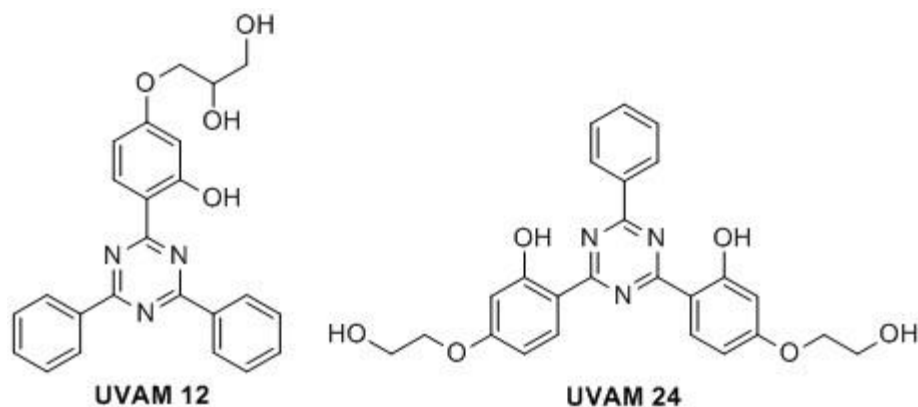


Figure 4. Chemical structures of UVAMs **12** and **24**.

UV Analysis of UVAMs

The UV absorbance spectra of UVAMs **12** and **24** are presented in Figure 5 together with the UV absorbance spectrum of Tinuvin 1577. The higher wavelength band is ascribed to the π - π^* intramolecular charge transfer transition and the lower wavelength band is attributed to localized π - π^* transitions. The UV profile of UVAM **12** mirrored that of Tinuvin 1577 because the chromophore in UVAM **12** is identical to the chromophore present in the commercial UV additive. Although DMSO is a polar solvent known to disturb the IMHBs of 2-hydroxybenzophenone (BP) and 2-(hydroxyphenyl)benzotriazole (BT) UV absorbers, there is no evidence of DMSO having an effect on the UV absorption profiles of these 2-(2-hydroxyphenyl)-1,3,5-triazine (TA) monomers, presumably due to their more robust IMHBs.

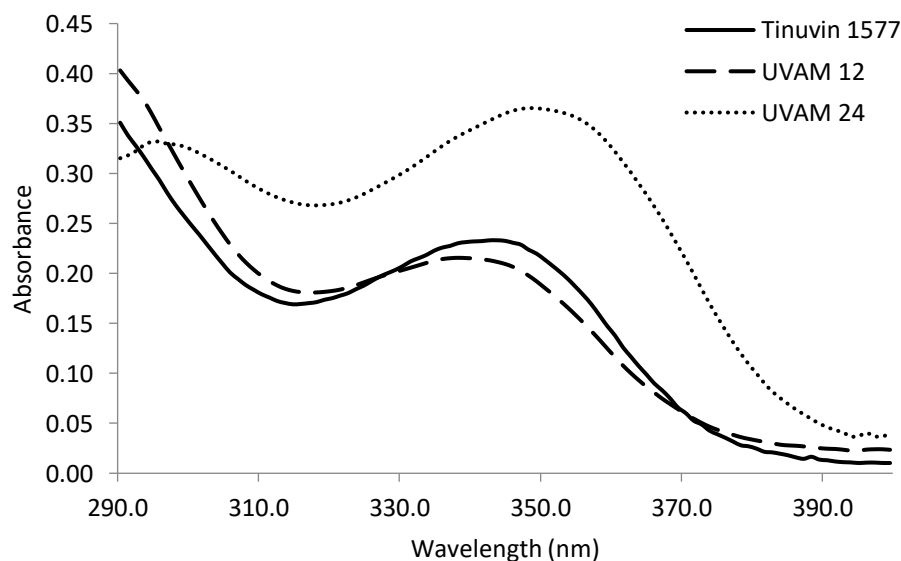


Figure 5. UV absorbance spectra of 0.1 mM solutions of Tinuvin 1577 (CHCl_3), UVAM **12** (DMSO) and UVAM **24** (DMSO).

Increasing the conjugation and the number of π bonds reduces the energy gap required for electron promotion. A red-shift is commonly observed since reducing the energy needed for excitation increases the λ_{max} . UVAM **24** had a higher molar extinction coefficient than Tinuvin 1577 and UVAM **12** throughout the 290-400 nm region. Increasing the number of resorcinyl moieties and the number of IMHBs caused a red-shift for

both the π - π^* and charge-transfer transitions. Dobashi^{34,35} established a clear relationship between the photostabilizing effect and the maximum wavelength of absorption (λ_{\max}) of the UVA. Dobashi demonstrated that BP and BT ultraviolet absorbers with higher λ_{\max} were the superior photostabilizers. If the same is true for TA derivatives, and absorbance at longer wavelengths enhances the photostabilizing effect, then this underlines the potential of UVAM **24**. Furthermore, due to its higher λ_{\max} , UVAM **24** is expected to be better at preventing the formation of the fluorescent by-products formed by light with wavelengths in the range 310-360 nm.^{7,9}

Synthesis and characterization of PET Copolymers

The polyesters in this study were synthesized on a 100 g scale using *bis*(2-hydroxyethyl) terephthalate) (BHET) (Figure 6), and they contained identical molar equivalents of Tinuvin 1577, UVAM **12** and UVAM **24** in the monomer feed (Table 1). The transesterifications generated ethylene glycol as a by-product, which was removed by vacuum. A sudden and significant increase in viscosity was observed during the syntheses, whereby the stirrer revolution rate dropped by 30-40 rpm due to the crystallization of the PET chains. The sudden increase in viscosity was used to judge the end points of the polymerizations, at which point the polymers were extruded into ice-cold water.

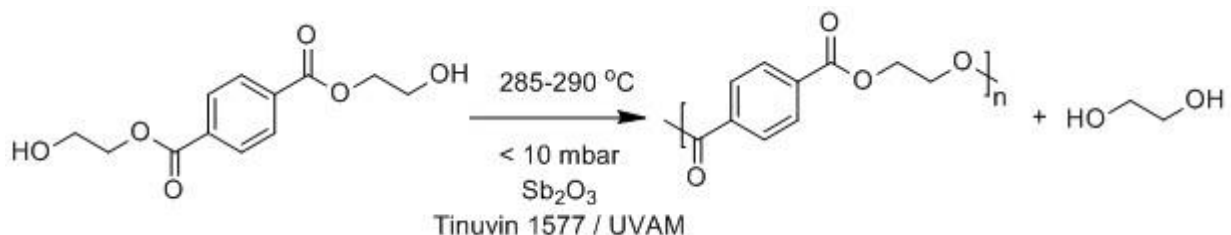


Figure 6. Polymerization of BHET in the presence of Tinuvin 1577/UVAM to yield PET and ethylene glycol with the UV absorber being either physically mixed (Tinuvin 1577) or chemically bound (UVAM) into the PET.

Table 1. Levels of Tinuvin 1577/UVAM present, and T_g , T_m , \overline{M}_w , \overline{D} and average thickness of PET films

Polymer	UVAM/Tinuvin (mol %)	\overline{M}_w (g/mol)	\overline{D}	T_g (°C)	T_m (°C)	Average Film Thickness (μm)
PET	0	11,750	3.3	77	256	48.1
PET (Tinuvin 1577)	0.60	14,350	3.4	78	257	60.0
Poly(ET-co-UVAM 12)	0.60	11,750	3.4	76	256	38.2
Poly(ET-co-UVAM 24)	0.60	11,550	3.4	75	253	53.6

The polymers synthesized in the polycondensation PC rig were moulded into cast films (width 6 cm, length 6 cm, thickness 0.1 cm) using a thermal press. These cast films were stretched biaxially on a T. M. Long Stretcher³⁶ at Wilton to give films with average thicknesses in the range 38.2-60.1 μm . The polymers were held above their glass transition temperature (105 °C) for 15 seconds and stretched biaxially. Biaxial stretching aligns the polymer chains and improves mechanical strength in both the transverse and longitudinal directions. Differential scanning calorimetry (DSC) analysis showed that the films had similar T_g , T_m and degree of crystallinity. Cast films which were held for longer than 15 seconds at 105 °C tended to crack due to crystallization beginning to take place before stretching. Gel Permeation Chromatography (GPC) analysis showed a 5-10% decrease in the molar mass of the polymers due to some thermal degradation taking place

during thermal processing at 275 °C. Reducing the extent of thermal degradation was possible by simply compressing the films at lower temperatures, such as 260-265 °C, but this had a detrimental effect on the quality of the films which failed to stretch due to the presence of air pockets.

UV analysis of polymers and solvent extracts

The UV absorbance spectra of the polymer films (Figure 7) showed PET (Tinuvin 1577) and Poly(ET-co-UVAM **12**) as having similar UV profiles, whereas Poly(ET-co-UVAM **24**) exhibited higher molar absorptivity within the 320-400 nm region. The higher molar extinction coefficient of Poly(ET-co-UVAM **24**) was attributed to the presence of UVAM **24**. None of the UV spectra showed signs of protrusion into the visible region.

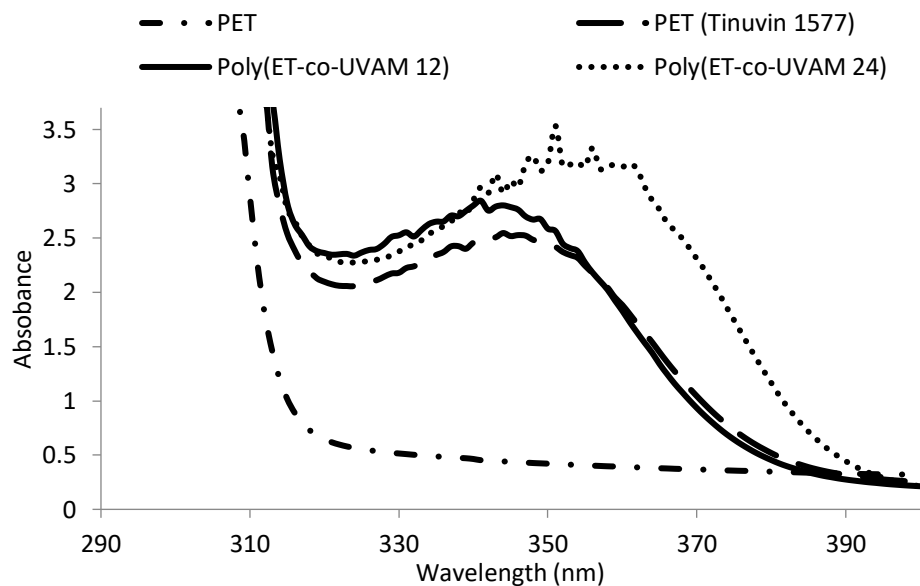


Figure 7. UV absorbance spectra of polymer films: PET, PET with Tinuvin 1577, Poly(ET-co-UVAM **12**) and Poly(ET-co-UVAM **24**).

Solvent extraction tests were carried out to investigate the potential leaching of stabilizer from the polymer matrices. CHCl_3 was used as an extraction solvent in a Soxhlet extraction set-up, and the chloroform extracts were analyzed using UV-Vis spectroscopy.

The UV spectra of the chloroform extracts showed that Tinuvin 1577 was susceptible to being washed out of the PET by chloroform (chloroform is a non-solvent for PET) and that the polymer bound UVAMs were resistant to solvent extraction (Figure 8). Using the molar extinction coefficient of Tinuvin 1577 ($\epsilon = 23,000 \text{ L mol}^{-1} \text{ cm}^{-1}$), 84% of the additive was calculated to have migrated into the solvent by the end of the Soxhlet extraction process. The rate of leaching of Tinuvin 1577 in the solvent extraction study is not comparable to the rate of leaching that will occur in a weatherometer, whereby Tinuvin 1577 would be expected to migrate out of the polymer at a much slower rate during a typical weathering process.

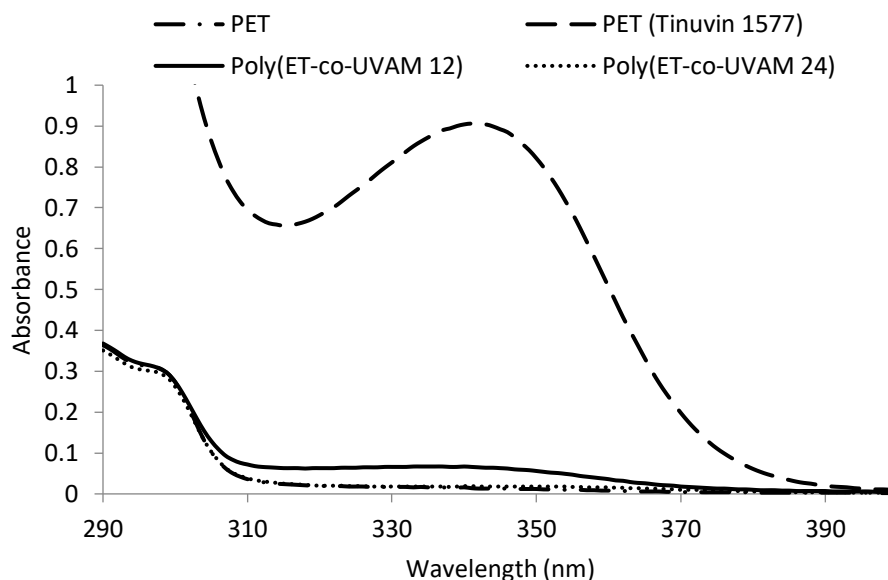


Figure 8. UV absorption spectra of solvent extracts after solvent extraction of PET films.

Weathering of PET Films

Polymer films containing the various stabilizers were weathered in a QUV-A weatherometer and analyzed periodically by ATR FT-IR spectroscopy and GPC. The films were weathered for a total of 1082 hours (45 days), with the exception of the PET control P27 which was removed from the weatherometer after becoming extremely brittle after 859 hours. The stabilized films exhibited wrinkles and became noticeably more brittle after 653 hours. None of the films displayed any yellowing to the eye after weathering.

ATR FT-IR spectroscopy measurements were carried out on the front surface of each film at regular intervals between 0 and 1082 hours of UV exposure. This technique analyzes the first 2-3 microns of the film surface and thus emphasizes the oxidative degradation more than the anaerobic degradation. Day and Wiles²⁸ monitored surface degradation of PET by using a height ratio of the bands at 3290 and 2970 cm^{-1} , assigned to the carboxylic acid O-H stretch and the aliphatic C-H stretch, respectively. The C-H vibration for the present films appeared at 2960 cm^{-1} , so the ratios were calculated using this wavenumber instead of 2970 cm^{-1} (Figure 9). The values plateaued for each sample once the penetration depth of the ATR became saturated with COOH functional groups. In a fashion similar to results reported by Day and Wiles, a rapid increase in COOH formation preceded a plateau for the PET control. PET (Tinuvin 1577) and Poly(ET-co-UVAM **12**) displayed similar behavior to the control, although at a slower rate, and Poly(ET-co-UVAM **24**) had the slowest rise in COOH formation, which was credited to the presence of UVAM **24**.

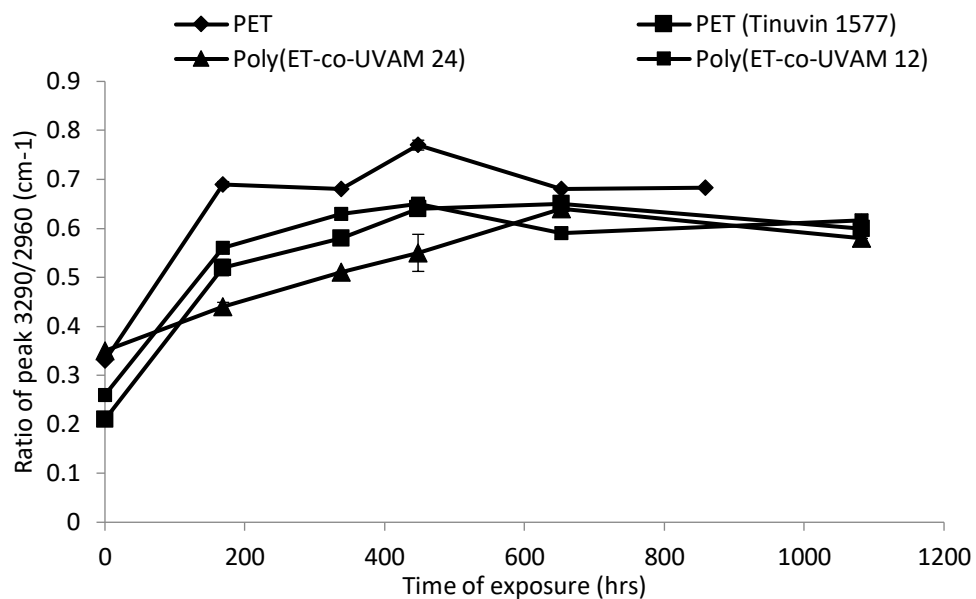


Figure 9. ATR FT-IR ratios of 3290/2960 cm⁻¹ bands for unstabilized and stabilized PET films.

The GPC analysis supports the FT-IR measurements, with the PET control polymer degrading the fastest whilst UVAM **24** was the most effective additive at preventing chain scissions in the bulk and at the surface of the polymer.

The weight average molecular weight (\overline{M}_w) of unstabilized PET was found to increase rapidly and was a clear sign of crosslinking, which was evident from the extreme brittleness of the PET control after 859 hours (Figure 10). The presence of Tinuvin 1577, UVAM **12** and **24** resulted in a slow decrease in both the \overline{M}_w and number average molecular weight (\overline{M}_n) which showed that the UV absorbing stabilizers were effective in combating crosslinking and that chain scissions were the main product of degradation in the stabilized films.

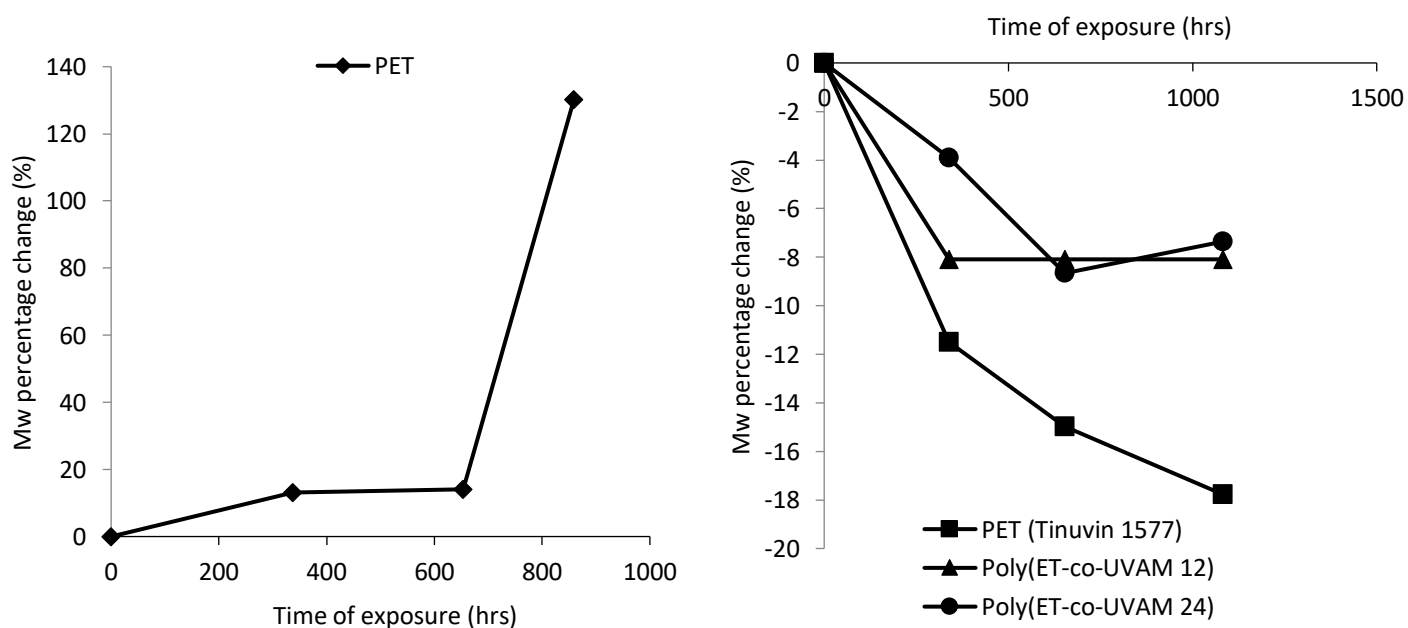


Figure 10. Plot of percentage change in \overline{M}_w against hours of exposure for PET (left) and stabilized films (right).

The percentage change in \overline{M}_w and \overline{M}_n as a function of time of exposure show that the UVAMs **12** and **24** offered greater UV protection than Tinuvin 1577. PET (Tinuvin 1577) showed the most rapid decrease in \overline{M}_w and \overline{M}_n for the stabilized films and a continuous fall after 338 hours. The \overline{M}_w of the UVAM stabilized PET films reached a plateau at 859 hours after a loss of 8-11%. Poly(ET-co-UVAM **24**) showed a slight increase in \overline{M}_w at 1082 hours with respect to the \overline{M}_w at 859 hours due to the degree of crosslinking overtaking the impact of chain scissions. Poly(ET-co-UVAM **24**) also exhibited the slowest decrease in \overline{M}_w and \overline{M}_n which is in agreement with the FT-IR surface analysis. In this study, UVAM **24** was the most effective stabilizer for preventing chain scissions in both the bulk and the surface of the polymer.

The PET control displayed a rapid rise in molar mass dispersity as crosslinking increased the \overline{M}_w and the chain scissions decreased the \overline{M}_n (Figure 11). The FT-IR analysis of the control showed high levels of chain scissions at the surface which also played a large role in reducing the \overline{M}_n . The molar mass dispersity increased at a much slower rate for the stabilized PET films due to the UV absorbers effectively slowing the rate of crosslinking and chain scissions. A decrease in both \overline{M}_w and \overline{M}_n showed that the main outcome of degradation for the stabilized films was chain scissions and that crosslinking was playing a smaller role in comparison to the PET control. The UVAMs limited the chain scissions more effectively than Tinuvin 1577, which led to a slower increase in the molar mass polydispersity of Poly(ET-co-UVAM **12**) and Poly(ET-co-UVAM **24**) compared to PET (Tinuvin 1577).

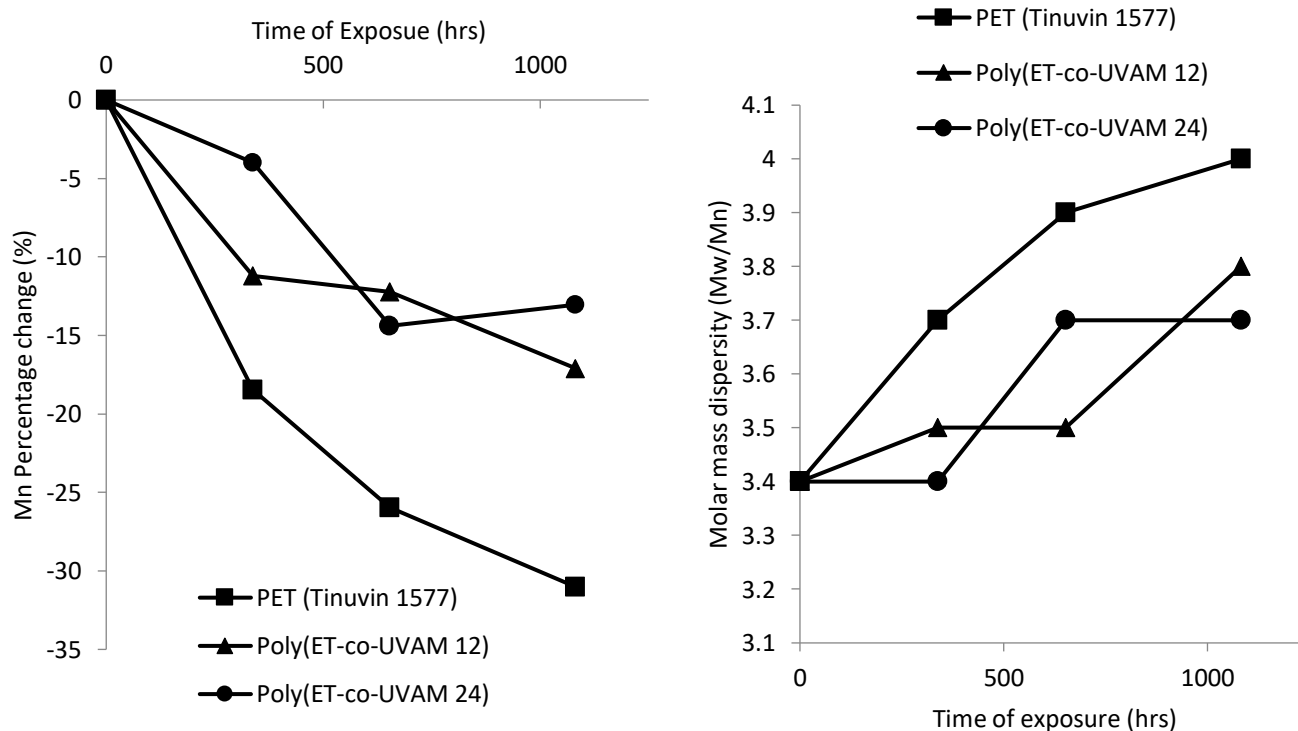


Figure 11. Plot of percentage change in the \overline{M}_n (left) and molar mass polydispersity (right) against hours of exposure for stabilized PET films (excluding PET control).

Wang postulated that the average degree of degradation ($\bar{\alpha}$) was related to the \overline{M}_n at 0 hours and at time t hours of exposure (\overline{M}_{nt}) (Equation 1). This equation can be rearranged to obtain the number of chain scissions per molecule (S) (Equation 2).

$$\bar{\alpha} = \frac{S}{\overline{M_{n0}}} = \frac{1}{\overline{M_{nt}}} - \frac{1}{\overline{M_{n0}}}$$

Equation 1. Calculation of average degree of degradation ($\bar{\alpha}$) using the number of chain scissions per molecule (S), number average molecular weight at 0 hours of exposure ($\overline{M_{n0}}$) and number average molecular weight at t hours of exposure ($\overline{M_{nt}}$).

$$S = \frac{\overline{M_{n0}}}{\overline{M_{nt}}} - 1$$

Equation 2. Calculation of number of chain scissions per molecule (S) using the number average molecular weight at 0 hours of exposure ($\overline{M_{n0}}$) and number average molecular weight at t hours of exposure ($\overline{M_{nt}}$).

Plotting S against exposure time further reinforced the conclusion that the UVAMs were more effective than Tinuvin 1577 in preventing chain scissions during UV degradation (Figure 12). Similarly to the observations by Wang and Lawrence, the films showed a two-step degradation process with a rapid rise in chain scissions of 'weak links' between 0 and 338 hours followed by a slower rise in chain scissions of the remaining 'normal links' after 338 hours. The polymerized UVAMs resulted in a slower rise in chain scissions for both the initial and later phases of UV degradation compared to the commercial additive. UVAM **24** was the most effective stabilizer at preventing 'weak link' and 'normal link' chain scissions, so much so that after 653 hours crosslinking begins to take a more prominent role than chain scissions in Poly(ET-co-UVAM **24**).

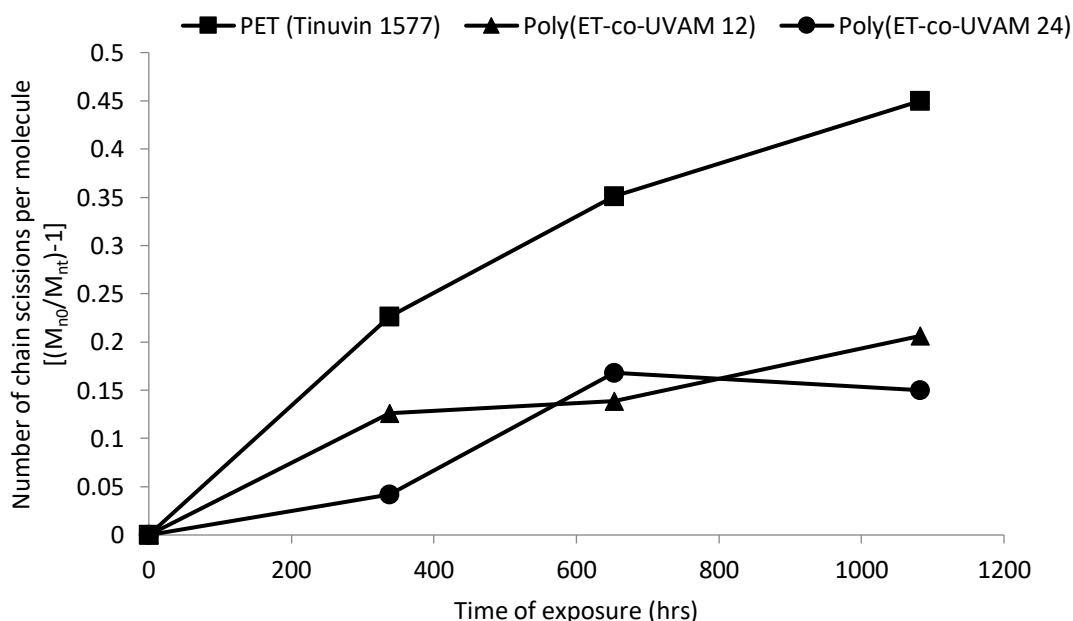


Figure 12. Plot of number of chain scissions per molecule against hours of exposure for stabilized PET films (excluding PET control).

A critical point to make is that UVAM **12** mimicked both the UV profile and the thermal stability of Tinuvin 1577, thus comparing the superior photostabilizing effect of UVAM **12** with that of Tinuvin 1577 demonstrates that polymerizing UV absorbers into the polymer chain offers a greater protection against UV degradation.

Furthermore, the UVAMs outperform the commercial additive in both the early and later stages of UV degradation. Since leaching from the polymer matrix takes time, one would expect the UVAMs to offer greater stabilization than the commercial additive primarily in the latter stages of weathering by which point in time a portion of Tinuvin 1577 has been lost to leaching. However, the superiority of the UVAMs over Tinuvin 1577 in the early stages of weathering as well suggests that the UVAMs possess other useful advantages over admixed commercial stabilizers in addition to higher leaching resistance, such as increased thermal resistance and lower volatility.

As mentioned previously, one other disadvantage of using Tinuvin 1577 as a UV stabilizer is that the volatile commercial additive fumes during processing which creates difficulties when handling industrial scale processing and leads to a loss of stabilizer. An argument can be made that the dominance of the UVAMs over Tinuvin 1577 in the initial phase of degradation may indicate that there are higher levels of UVAMs in the polymer despite employing equal loadings in the feed. The higher levels of UVAM can arise from circumventing loss from fuming by covalently tethering of the UV stabilizer to the polymer. This provides a possible explanation for the slower rates of degradation in the initial stages UV exposure for Poly(ET-co-UVAM **12**) and Poly(ET-co-UVAM **24**), with respect to PET (Tinuvin 1577). Employing the less volatile UVAMs would reduce waste and cost, as well as increase the ease of handling for large scale processes.

The UVAMs become increasingly impressive in the second phase of degradation, with Poly(ET-co-UVAM **12**) and Poly(ET-co-UVAM **24**) reaching a plateau whereas the number of chain scissions continued to rise for PET (Tinuvin 1577). The effect of leaching is expected to become even more prominent in the latter stages of degradation which ultimately leaves PET (Tinuvin 1577) increasingly vulnerable to photodegradation. The covalently tethered UVAMs remain locked in the polymer matrix and offer Poly(ET-co-UVAM **12**) and Poly(ET-co-UVAM **24**) enhanced levels of protection over an extended time period.

Considering both the FT-IR and GPC analyses, UVAM **24** was unquestionably the most effective stabilizer in this degradation study. One simple explanation for this is the higher molar extinction coefficient throughout the 290-400 nm region for **24** in comparison to both **12** and Tinuvin 1577. Dobashi^{34,35} postulated that ultraviolet absorbers with higher λ_{\max} were the superior photostabilizers, and reported that the strength of absorbance only comes into play for UVAs with the same λ_{\max} . In this case, the UVA with the higher ϵ was the superior stabilizer. This explains the excellent performance of UVAM **24** which has a higher λ_{\max} and a higher molar absorptivity compared to Tinuvin 1577 and UVAM **12**.

Conclusions

UVAMs were successfully polymerized into PET at 0.6 mol % loadings without significantly affecting the glass transition temperature, melting temperature and molar mass of the polymers. Solvent extraction experiments on UV-stabilized PET films showed the tendency for Tinuvin 1577 to leach out of the polymer matrix whereas the covalently anchored UVAMs did not show any sign of migration; this emphasizes a significant advantage of using UVAMs over conventional non-polymerizable UV absorbing additives.

ATR FT-IR spectroscopic analysis showed that the films containing UVAM **24** were the most effective at slowing the increase in carboxylic acid group formation at the surface of PET films. The copolymers incorporating UVAMs **12** and **24** showed the slowest increase in the rate of chain scissions at the surface. A PET control showed the most rapid increase in chain scissions followed by a plateau once the depth of ATR penetration became saturated with COOH groups. Films containing Tinuvin 1577 and UVAM **12** showed similar behavior to the PET control, albeit at a slower rate of COOH production.

GPC analysis supported the FT-IR study conclusions in a number of ways, with the PET control showing the most rapid rate of degradation. Crosslinking was the major photodegradation product for the PET control whilst chain scissions were the primary photodegradation product of the stabilized films. The stabilized films displayed a decrease in the \overline{M}_w and \overline{M}_n , with the UVAMs significantly outperforming Tinuvin 1577 in both the initial and latter stages of degradation.

UVAM **12** was used as direct comparison to Tinuvin 1577 since they had essentially identical UV profiles and thermal stabilities. The impressive performance of UVAM **12** demonstrated that polymerizing UV absorbers into the polymer matrix was more effective than simply employing an additive, and circumvents any fuming issues during processing as well. UVAM **24** was the most effective stabilizer of all the stabilizers evaluated in this study; it suppressed chain scissions very effectively at both the surface and the interior of PET films.

Experimental Section

General. BHET and Sb_2O_3 were sourced from Aldrich and Tinuvin 1577 was sourced from BASF. The polymers were synthesized in a polycondensation (PC) rig at DuPont Teijin Films, Wilton, UK. The equipment included a polycondensation head, stirrer guide, air stirrer, delivery side-arm, distillate tube inside an ice-filled Dewar flask, thermocouples and optical revolution counter. The system was connected to a gas and vacuum manifold. The polymers synthesized in the PC rig were moulded into cast films (width 6 cm, length 6 cm, thickness 0.1 cm) using a thermal press at Strathclyde University. A combination of a steel mold, steel plates, aluminum sheets and poly(tetrafluoroethylene) (PTFE) baking paper were used to sandwich the polymer. The polymers were compressed (35 kg/cm^2) at a temperature of $275 \text{ }^\circ\text{C}$. The cast films were stretched biaxially on a T. M. Long Stretcher at DTF in Wilton. The polymer was held at $105 \text{ }^\circ\text{C}$ for 15 seconds before stretching biaxially at a rate of 2.54 cm/sec to give approximately $14 \times 14 \text{ cm}$ film. The thickness of the films was measured using a Sylvac D100S digital unit. UV-Visible absorption spectra of the polymer films were recorded using a Shimadzu UV-1800 UV spectrophotometer. Solution state UV-Visible absorption spectra were acquired using a Photonics CCD array UV-VIS spectrophotometer with a 1 mm pathlength quartz cell. DMSO and CHCl_3 were used as solvents and the scan range was 290-500 nm. Soxhlet extraction was carried out using CHCl_3 (200 mL) and 0.5 g of polymer for 24 hours. The extraction solvent was transferred to a 250 mL volumetric flask, made up to the volumetric mark and analyzed using UV-Vis spectroscopy. ATR FT-IR measurements were carried out on a Thermo Scientific Nicolet iS50 FT-IR Spectrometer at a spectral resolution of 4 cm^{-1} , averaged over 32 scans. A piece of filter paper was placed on top of all thin film samples to ensure even and complete contact was made between the film and the diamond. An 'Advanced ATR Correction' algorithm, provided within the software supplied, was used to correct the data (as recommended by Thermo Fisher Scientific, Hemel Hempstead) before analysis was carried out. A ratio of the peak heights at 3290 cm^{-1} (O-H stretch of COOH) and 2960 cm^{-1} (C-H stretch reference peak) with a baseline from 4000 cm^{-1} and 400 cm^{-1} was used. The PET films were subjected to UV degradation using a QUV accelerated weathering instrument under UV-A radiation in accordance with the ISO 4893-3 standard. The weathering cycle consisted of 8 hours of continuous UV luminescence at 0.76 Wm^{-2} (340 nm) at $60 \text{ }^\circ\text{C}$ followed by 4 hours of dark condensation at $50 \text{ }^\circ\text{C}$. TGA of UVAMs was performed using a Perkin Elmer TGA 7. Approximately 10 mg of sample was heated under air at a rate of $10 \text{ }^\circ\text{C/min}$ from $40 \text{ }^\circ\text{C}$ to $500 \text{ }^\circ\text{C}$. Thermal analyses of polymer samples were carried out using a 6000 Enhanced Single-Furnace Differential Scanning Calorimeter (DSC). The samples were heated from $-20 \text{ }^\circ\text{C}$ to $310 \text{ }^\circ\text{C}$ at a rate of $20 \text{ }^\circ\text{C/min}$, cooled back to $-20 \text{ }^\circ\text{C}$ at a rate of $50 \text{ }^\circ\text{C/min}$ and reheated to $310 \text{ }^\circ\text{C}$ at a rate of $20 \text{ }^\circ\text{C/min}$. The molar masses of the polymers were determined using Gel Permeation Chromatography (GPC) which was carried out at Smithers Rapra Limited on a

Malvern/Viscotek TDA 301 instrument with a refractive index detector. The samples were dissolved (2 mg/mL) in hexafluoroisopropanol (HFIP), filtered through a 0.45 μm membrane and passed through an Agilent PL HFIP Gel Column at a flow rate of 0.8 mL/min at 40 °C.

General synthesis of poly(ET-co-UVAMs). A stirred slurry of BHET, UVAM/Tinuvin 1577 and Sb_2O_3 (0.15 g, 0.52 mmol) was added into a polycondensation rig glass tube. The glass tube was scored lightly on the stem, using a Stanley blade, to facilitate the stem being broken off for extrusion of the final polymer, and clamped inside a heating block. The glass tube was fitted with a polycondensation head, stirrer guide, air stirrer, delivery side-arm, distillate tube inside an ice-filled Dewar flask, thermocouples, optical revolution counter and connected to a gas manifold. The temperature was raised using a control box to 230 °C over 60 mins under a nitrogen purge. The air stirrer was then started with a pressure of 9.5 psi, with the stirrer speed reaching 175 rpm. After stirring under a nitrogen purge at 230 °C for 30 mins, the system was put under vacuum. The pressure was reduced gradually to less than 3 mbar as the temperature was increased to 290 °C at a rate of 1 °C/min. Once the stirrer speed dropped by 30-40 rpm, the polymerization was judged to be complete and the vacuum was replaced slowly with a nitrogen purge. A hammer and chisel were used to break the stem of the PC rig tube, and the synthesized copolymer was extruded and quenched into an ice-water bath. The copolymer lace formed was left to dry in air.

Polymer film production. The polymer fibers were molded into a cast film using a thermal press. The polymer fibers were cut into small pieces using scissors and 7 grams of polymer cuttings were placed between two layers of PTFE baking paper (9 cm x 9 cm) which was positioned in the middle of a steel mold (width 6 cm, length 6 cm, height 0.1 cm). This was sandwiched between two 0.1 mm thick aluminum sheets which, in turn, were sandwiched by two 1 mm thick steel plates. This was then placed in a thermal press at 275 °C and allowed to melt for 30 seconds. 35 kg/cm² of pressure was applied and released, repeating this 50 times to ensure all the air bubbles were released. The sandwich was removed from the press and dropped quickly into a bucket of iced water. The aluminum sheets and baking paper were peeled off to give a 1 mm thick cast polymer, 6 cm in length and 6 cm in width.

The cast film was stretched biaxially on a T. M. Long Stretcher at DTF in Wilton. The cast polymer was clipped onto draw arms (6 x 6 cm) inside an oven set at 105 °C. The polymer was held at this temperature for 15 seconds before stretching biaxially at a rate of 2.54 cm/sec to give 14 x 14 cm film.

Acknowledgements

The authors would like to thank DuPont Teijin Films Limited for funding the PhD studentship for Omer Can Erdemli.

References

1. Lee, C. O.; Chae, B.; Kim, S. B.; Jung, Y. M.; Lee, S. W. *Vib. Spectrosc.*, **2012**, 60, 142–145.
<https://doi.org/10.1016/j.vibspec.2011.10.013>
2. Keck, J.; Kramer, H.; Port, H. *J. Phys. Chem.*, **1996**, 100, 14468–14475.
<https://doi.org/10.1021/jp961081h>
3. Day, M.; Wiles, D. *J. Appl. Polym. Sci.*, **1972**, 16, 175–189.

- <https://doi.org/10.1002/app.1972.070160116>
4. Day, M.; Wiles, D. *J. Appl. Polym. Sci.*, **1972**, 16, 191–202.
<https://doi.org/10.1002/app.1972.070160118>
 5. Day, M.; Wiles, D. *J. Appl. Polym. Sci.*, **1972**, 16, 203–215.
<https://doi.org/10.1002/app.1972.070160118>
 6. Blais, P.; Day, M.; Wiles, D. *J. Appl. Polym. Sci.*, **1973**, 17, 1895–1907.
<https://doi.org/10.1002/app.1973.070170622>
 7. Fechine, G.; Rabello, M.; Souto-Maior, R. *Polym. Degrad. Stab.*, **2002**, 75, 153–159.
[https://doi.org/10.1016/S0141-3910\(01\)00214-2](https://doi.org/10.1016/S0141-3910(01)00214-2)
 8. Fechine, G.; Christensen, P.; Egerton, T.; White, J. *Polym. Degrad. Stab.*, **2009**, 94, 234–239.
<https://doi.org/10.1016/j.polymdegradstab.2008.10.025>
 9. Fechine, G.; Rabello, M.; Souto Maior, R.; Catalani L., *Polym. J.*, **2004**, 45, 2303–2308.
<https://doi.org/10.1016/j.polymer.2004.02.003>
 10. Rivaton, A.; Gardette, J.; Hoyle, C.; Ziemer, M.; Fagerburg, D.; Grossetête T., *Polym. J.*, **2000**, 41, 3541–3554.
[https://doi.org/10.1016/S0032-3861\(99\)00580-7](https://doi.org/10.1016/S0032-3861(99)00580-7)
 11. Catalan, J.; Valle, J.; Diaz, C.; Paz, L. *J. Phys. Chem. A*, **1999**, 103, 10921–10934.
<https://doi.org/10.1021/jp992631p>
 12. LeGourriérec, D.; Kharlanov, V.; Brown, R.; Rettig, W. *J. Photochem. Photobiol. A Chem.*, **2000**, 130, 101–111.
[https://doi.org/10.1016/S1010-6030\(99\)00206-3](https://doi.org/10.1016/S1010-6030(99)00206-3)
 13. Otterstedt, J. *J. Chem. Phys.*, **1973**, 58, 5716.
<https://doi.org/10.1063/1.1679196>
 14. Crawford, J. *Prog. Polym. Sci.*, **1999**, 24, 7–43.
[https://doi.org/10.1016/S0079-6700\(98\)00012-4](https://doi.org/10.1016/S0079-6700(98)00012-4)
 15. Kuila, D.; Kvakovszky, G.; Murphy, M.; Vicari, R.; Rood, M.; Fritch, K.; Fritch, J.; Wellinghoff, S.; Timmons, S. *Chem. Mater.*, **1999**, 11, 109–116.
<https://doi.org/10.1021/cm9805121>
 16. Prucker, O.; Naumann, C.; Rühle, J. *J. Am. Chem. Soc.*, **1999**, 121, 8766–8770.
<https://doi.org/10.1021/ja990962+>
 17. Rajan, V.; Wäber, R.; Wieser, J. *J. Appl. Polym. Sci.*, **2012**, 124, 4007–4015.
<https://doi.org/10.1002/app.34560>
 18. Rajan, V.; Wäber, R.; Wieser, J. *J. Appl. Polym. Sci.*, **2012**, 124, 3988–3995.
<https://doi.org/10.1002/app.33878>
 19. Mizutani, Y.; Kusumoto, K. *J. Appl. Polym. Sci.*, **1975**, 19, 713–717.
<https://doi.org/10.1002/app.1975.070190308>
 20. Vogl, O.; Albertsson, A.; Janovic, Z. *Polym. J.*, **1985**, 26, 1288–1296.
[https://doi.org/10.1016/0032-3861\(85\)90301-5](https://doi.org/10.1016/0032-3861(85)90301-5)
 21. Pasch, H.; Shuhaibar, K.; Attari, S. *J. Appl. Polym. Sci.*, **1991**, 42, 263–271.
<https://doi.org/10.1002/app.1991.070420130>
 22. Al-Mobasher, A.; Attari, S.; Pasch, H.; *Polym. Bull.*, **1991**, 26, 39–46.
<https://doi.org/10.1007/BF00299346>
 23. Bailey, D.; Tirrell, D.; Vogl, O. *J. Polym. Sci.*, **1976**, 14, 2725–2747.
<https://doi.org/10.1002/pol.1976.170141113>
 24. Bailey, D.; Vogl, O. *Rev. Macromol. Chem. Phys.*, **1976**, 14, 267–293.
<https://doi.org/10.1080/15321797608065772>

25. Stein, M.; Keck, J.; Waiblinger, F.; Fluegge, A. P.; Kramer, H. E.; Hartschuh, A.; Port, H.; Leppard, D.; Rytz, G. *J. Phys. Chem. A*, **2002**, 106, 2055–2066.
<https://doi.org/10.1021/jp012134k>
26. Bojinov, V. B.; *Polym. Degrad. Stab.*, **2006**, 91, 128–135.
<https://doi.org/10.1016/j.polymdegradstab.2005.04.019>
27. Bojinov, V. B.; Georgiev, N. I.; Marinova, N. V. *Sensors Actuators B Chem.*, **2010**, 148, 6–16.
<https://doi.org/10.1016/j.snb.2010.05.022>
28. Bojinov V. B.; Simeonov, D. B. *Polym. Degrad. Stab.*, **2010**, 95, 43–52.
<https://doi.org/10.1016/j.polymdegradstab.2009.10.012>
29. Bojinov, V. B.; Panova, I. P.; Simeonov, D. B. *Dye. Pigment.*, **2009**, 83, 135–143.
<https://doi.org/10.1016/j.dyepig.2008.10.007>
30. Bojinov, V. B.; Georgiev, N. I.; Bosch, P. J. *Fluoresc.*, **2009**, 19, 127–39.
<https://doi.org/10.1007/s10895-008-0394-2>
31. Bojinov, V. B.; Panova, I. P.; Simeonov, D. B. *Dye. Pigment.*, **2008**, 78, 101–110.
<https://doi.org/10.1016/j.dyepig.2007.10.010>
32. Bojinov V. B.; Panova, I. P. *Polym. Degrad. Stab.*, **2008**, 93, 1142–1150.
<https://doi.org/10.1016/j.polymdegradstab.2008.03.003>
33. Bojinov V. B.; Simeonov, D. B. *J. Photochem. Photobiol. A Chem.*, **2006**, 180, 205–212.
<https://doi.org/10.1016/j.jphotochem.2005.10.018>
34. Dobashi, Y.; Kondou, J.; Ohkatsu, Y. *Polym. Degrad. Stab.*, **2005**, 89, 140–144.
<https://doi.org/10.1016/j.polymdegradstab.2005.01.010>
35. Dobashi Y.; Ohkatsu, Y. *Polym. Degrad. Stab.*, **2008**, 93, 436–447.
<https://doi.org/10.1016/j.polymdegradstab.2007.11.011>
36. *Biaxial Stretching of Film: Principles and Applications*, M. T. DeMeuse M. T. (Ed.), Woodhead Publishing, Cambridge, **2011**
<https://www.sciencedirect.com/book/9781845696757/biaxial-stretching-of-film>

This paper is an open access article distributed under the terms of the Creative Commons Attribution (CC BY) license (<http://creativecommons.org/licenses/by/4.0/>)